

Applications of Three-Dimensional Discontinuous Deformation Analysis: A Review

S. Amir Reza Beyabanaki

McMillen Jacobs Associates, Walnut Creek, CA, USA

ABSTRACT: Discontinuous deformation analysis is a powerful numerical method to simulate the behavior of blocky structures. This study presents a review of applications of three-dimensional discontinuous deformation analysis. In this review paper, the applications are grouped into eight categories: (1) toppling analysis, (2) rockfall analysis, (3) landslides, (4) stability analysis of gravity dams, (5) magma transport through pre-existing fractures, (6) in-situ thermal test, (7) damage analysis of brick masonry buildings, and (8) tunnel stability. It is found that for the problems addressed by the papers in this review, three-dimensional discontinuous deformation analysis method performs well.

KEYWORDS: numerical modeling, discontinuous deformation analysis, three-dimensional, applications.

Date of Submission: 20-10-2019

Date of acceptance: 03-11-2019

I. INTRODUCTION

Two-Dimensional Discontinuous Deformation Analysis (2-D DDA) is a numerical method that was introduced by Shi [1, 2] to simulate large movements in discontinuum media to analyze the mechanical response of discrete blocks. Applications of this method and validation studies on the 2-D DDA are reviewed by MacLaughlin and Doolin [3], Ohnishi and Nishiyama [4], Hatzor and Bakon-Mazor [5], Ohnishi et al. [6], Ohnishi et al. [7], Yagoda-Biran and Hatzor [8], and Ning et al. [9].

Three-Dimensional Discontinuous Deformation Analysis (3-D DDA) is relatively young and was developed by Shi [10]. Yeung et al. [11] and Liu et al. [12] presented the basic formulations of 3-D DDA in detail. A point-to-face model for contacts between polyhedral blocks in 3-D DDA was developed by Jiang and Yeung [13]. Also, Wu et al. [14] developed a new contact searching algorithm for frictionless vertex-to-face contact problems. Moreover, Yeung et al. [15] and Wu [16] presented different algorithms for edge-to-edge contacts. Finally, a new algorithm to search and calculate geometrical contacts in 3-D was presented by Beyabanaki et al. [17]. Beyabanaki et al. [18] presented a new point-to-face contact algorithm for contacts between two polyhedral blocks with planar faces in 3-D DDA to improve the contact model. Also, Ahn and Song [19] presented a new contact definition algorithm for 3-D DDA. As the next step, block deformability in 3-D DDA was improved by Beyabanaki et al. [20, 21]. Furthermore, as an alternative method to improve block deformability in 3-D DDA, high-order displacement functions were used by Beyabanaki et al. [22, 23]. Beyabanaki et al. [24] and Bakun-Mazor et al. [25] studied the validity of the method in order to show the capability of polyhedral-based 3-D DDA to model dynamic problems. Beyabanaki and Bagtzoglou [26, 27] presented a formulation of the sphere-based 3-D DDA. Finally, Fan et al. [28] presented a three-dimensional dynamic deformation formulation based on the strain-rotation decomposition, and Wang et al. [29] resolved contact indeterminacy between convex polyhedral blocks.

Although 3-D DDA has been used for variety of practical engineering problems, to date, no review paper has been published on applications of this method. In this paper, applications of 3-D DDA are grouped in different categories and reviewed.

II. BASIC THEORY OF 3-D DDA

3-D DDA is an implicit technique and involves formulation and solution of a system of simultaneous equilibrium equations. In this method, the total potential energy is the summation of all potential energy sources for each block, which involves the potential energy contributed by the point loads on a block, inertia forces, volume forces, fixed points, and potential energy when the blocks contact each other. In 3-D, there are six types

contacts (i.e., vertex-to-face, vertex-to-edge, vertex-to-vertex, face-to-face, edge-to-edge, and edge-to-face), and in 3-D DAA, they are transformed into the form of point-to-face contacts using a contact face [17]. Figure 1 shows concept of the point-to-face contact in 3-D DDA.

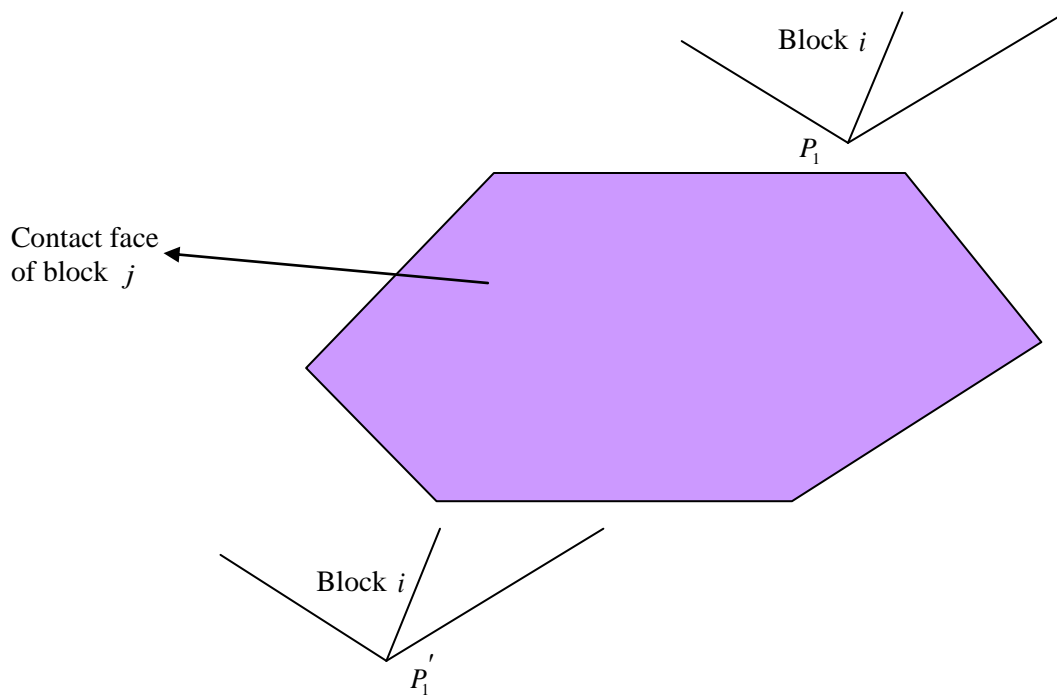


Fig.1. Point-to-face contact (adapted from Beyabanaki et. al. [18])

In 3-D DDA, the relation between blocks can be presented as below [17]:

$$\begin{Bmatrix} u \\ v \\ w \end{Bmatrix} = [T_i(x, y, z)] \cdot \{D_i\} \tag{1}$$

where

$$[T_i(x, y, z)] = \begin{bmatrix} 1 & 0 & 0 & -(y - y_0) & 0 & (z - z_0) & (x - x_0) & 0 & 0 & (y - y_0)/2 & 0 & (z - z_0)/2 \\ 0 & 1 & 0 & (x - x_0) & -(z - z_0) & 0 & 0 & (y - y_0) & 0 & (x - x_0)/2 & (z - z_0)/2 & 0 \\ 0 & 1 & 1 & 0 & (y - y_0) & -(x - x_0) & 0 & 0 & (z - z_0) & 0 & (y - y_0)/2 & (x - x_0)/2 \end{bmatrix} \tag{2}$$

and

$$\{D_i\} = (u_0, v_0, w_0, r_x, r_y, r_z, \epsilon_x, \epsilon_y, \epsilon_z, \gamma_{xy}, \gamma_{yz}, \gamma_{zx})^T \tag{3}$$

In the above-mentioned equations, \$(x_0, y_0, z_0)\$ is the coordinates of the block center, and \$(u_0, v_0, w_0)\$ represents rigid body translations; \$(r_x, r_y, r_z)\$ indicates the rotation angles in radians of block \$i\$ with a rotation centre at \$(x_0, y_0, z_0)\$. \$[T_i(x, y, z)]\$ is the first order displacement function, and \$\{D_i\}\$ is the vector of displacements of block \$i\$ in three dimensions.

The total potential energy for an N blocks system can be expressed in matrix form as follows [17]:

$$\begin{bmatrix} [K_{11}] & [K_{12}] & [K_{13}] & \dots & [K_{1N}] \\ [K_{21}] & [K_{22}] & [K_{23}] & \dots & [K_{2N}] \\ [K_{31}] & [K_{32}] & [K_{33}] & \dots & [K_{3N}] \\ \vdots & \vdots & \vdots & \ddots & \vdots \\ [K_{N1}] & [K_{N2}] & [K_{N3}] & \dots & [K_{NN}] \end{bmatrix} \begin{Bmatrix} \{D_1\} \\ \{D_2\} \\ \{D_3\} \\ \vdots \\ \{D_N\} \end{Bmatrix} = \begin{Bmatrix} \{F_1\} \\ \{F_2\} \\ \{F_3\} \\ \vdots \\ \{F_N\} \end{Bmatrix} \tag{4}$$

where $\{D_i\}$ and $\{F_i\}$ indicate displacement variables, and loading and moments caused by the stresses and external forces acting on block i , respectively. The stiffness submatrices $[K_{ij}]|_{i=j}$ depend on the material properties of block i , and $[K_{ij}]|_{i \neq j}$ is defined by the contacts between blocks i and j . The equilibrium equations for each time step are derived by minimizing the total potential energy. The total potential energy Π is the summation over all potential energy forms calculated as below:

$$\Pi = \pi_e + \pi_{is} + \pi_p + \pi_b + \pi_i + \pi_C + \pi_n + \pi_s + \pi_f \tag{5}$$

Where:

π_e = the potential energies due to disk stiffness;

π_{is} = the potential energy due to initial stress;

π_p = the potential energy due to point loading;

π_b = the potential energy due to body force;

π_i = the potential energy due to inertia forces;

π_C = the potential energy due to constrained spring;

π_n = the potential energy due to normal contact;

π_s = the potential energy due to shear contact; and

π_f = the potential energy due to friction force.

The simultaneous equations are derived by minimizing the total potential energy Π of the disk system[17]:

$$\begin{aligned} [K_{ij}] &= \frac{\partial^2 \Pi}{\partial d_{ir} \partial d_{js}} \quad , \quad r, s = 1, 2, 3 \\ \{F_i\} &= -\frac{\partial \Pi(0)}{\partial d_{ir}} \quad , \quad r = 1, 2, 3 \end{aligned} \tag{6}$$

where 0 refers to the initial state of each time state.

III. APPLICATIONS OF 3-D DDA

3-D DDA has different applications in engineering. Applications of this method are presented below.

3.1. Toppling Analysis

Hwang et al. [30] and Wu et al. [31] used 3-D DDA to investigate its applicability to simulate the failure process of a rock slope at the Amatoribashi-Nishi site in Japan. The toppling failure process was recorded by video. For this purpose, they simplified the geometry of the main blocks of the slope and created the 3D geometric model. They used the rock and joint physical properties obtained from the laboratory uniaxial compression tests, Brazilian tests, and direct shear tests. They compared the simulation results with the corresponding images taken on the video. The comparison of the simulation and the recorded behavior shows that the toppling behavior of the unstable block has been successfully simulated. However, the simulated movement of the unstable block was slightly different from the one in the field because of the oversimplification of the slope.

3.2. Rockfall Analysis

Several researchers have used 3-D DDA to analyze rockfall problems. Chen et al. [32, 33] compared 2D and 3D DDA in rockfall analysis and showed barrier effect of trees can be estimated by 3-D DDA simulation, which is impossible by using 2D program in terms of providing detailed spatial distribution. Also, the results showed that 2-D DDA simulations have better efficiency for slopes dominated by valleys and ravines. They verified the capability of DDA to model rockfalls by investigating the four basic types of motion involved in rockfall (i.e., free fall, sliding, rolling, and bouncing). Also, they incorporated GIS into the 3-D DDA program to generate a complicated slope modeling. However, the presented examples were not real problems.

Sasaki et al. [34] analyzed an actual rockfall of a volcanic mountain of height 1300 m. The distance from the mountain top to the national road is about 6000 m and the authors constructed a model with a width of 1000 m, height 1300 m and length of slope of 5500 m from the mountain top to the national road. The number of rocks was 200 and the block size was 20 m × 20 m × 20 m. The falling blocks were settled on the middle part of the slope. However, actual falling block size was estimated to be smaller than in the calculation.

Zheng et al. [35] incorporated GIS into the 3-D DDA program to investigate the effect of the 3D shape of falling rock blocks. The results show that the rounder the rock block is, the smaller the dispersion of rockfall is.

Sasaki et al. [36] introduced the fixed block option in 3-D DDA and showed it is effective for producing numerical stability and in saving calculation time. They used their technique to analyze rockfalls. They studied rockfalls due to an earthquake and heavy rainfall. In the first case, they assumed two block sizes of 25m×20m×5m (25 blocks) and 5m×5m×5m (75 blocks) to model the rockfall occurred due to an earthquake (M.6.8) in 2004 near the Shinano River in Japan. They could obtain acceptable falling distance of rockfalls from the modeling. However, they did not present quantitative comparison between the results and actual data. In the second analysis, they studied a rockfall due to a heavy rainfall. The size of the rock blocks was distributed between 2 and 6 m and the average size was 2.5 m. The slope was inclined 30 to 40 degrees downward. The obtained falling distances were close to the observations.

3.3. Landslides

Shi [37, 38] performed the stability analysis of the major block of a dam abutment using 3-D DDA. He also used Block Theory method and compared the results obtained from the two methods. Both block theory and 3-D DDA had the same result. The factor of safety was changing from 1.10 to 1.35 depend upon the assumption on the friction angles of two sliding faces. Figure 2 shows the sliding of the major key block under the gravity load computed by 3-D DDA.

Wang et al. [39] coupled 3-D DDA and the Smoothed Particle Hydrodynamics (SPH) to model the interaction between the solid and fluid phases to be used for simulating the landslide mass motion. For this purpose, they discretized the fluid into particles in the SPH method and used the Navier–Stokes equations to solve the flow. 3-D DDA was used to model the solids bounded by flat polygons. To verify the proposed method, they performed some numerical tests. In the tests, impulsive waves were generated by a wedge that slid along an inclined plane. They showed that the coupled 3-D DDA-SPH method could accurately capture both the wedge motion and the wave profiles during the whole solid–fluid interaction process and can be applied to landslide-generated impulsive waves.

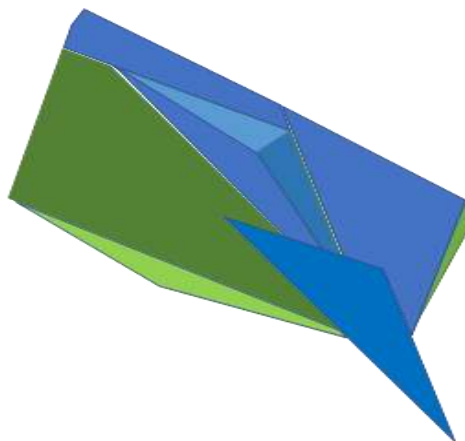


Fig.2. Sliding of major key block computed by 3-D DDA(adapted from [38])

Wang et al. [40] used the coupled 3-D DDA-SPH to solve the landslide-river interaction problem during the formation and failure of a landslide dam. They considered the kinematic characteristics of both the landslide and the water flow and showed that the coupled 3-D DDA-SPH method can well model the landslide-river interaction in the landslide dam simulation. Three scenarios were studied for the kinematic characteristics of the dam behavior: (1) still river flow, (2) river flow with high velocity, and (3) river flow with low velocity. The results showed that in case of the still river flow, the landslide can block the river once the geomorphological requirement is satisfied. The authors also considered a larger landslide mass (1.5 times larger) and concluded that the landslide with larger mass is much easier, and efficient to block the river flow and thus form the landslide dam with the same kinematic characteristics for both the landslide and river flow.

Wang et al. [41, 42] applied 3-D DDA for modeling landslide movement over complicated 3D topography. For this purpose, they presented a method to generate complicated topographies that can be incorporated in the block system Method. They demonstrated the applicability and performance of the proposed approach in dealing with the landslide movement over 3D topography and presented an example including a slope with rather complex terrain. They presented the results of the landslide movement sequence but did not verify the results.

Jing et al. [43] studied two factors that influence the slope failure pattern: (1) boundary condition: free lateral boundary and fixed lateral boundary, and (2) dip angle of discontinuity sets: 30° , 60° , and 90° . Figure 3 schematically shows the initial configuration of the 3-D DDA model with free lateral condition used in this study. The authors concluded that change of dip angle of discontinuity set has great influences on the slope failure, like the change from slide-toppling to sliding. Also, the failure pattern changes from toppling mixed with sliding to toppling with increasing of dip angle of basal joint sets. Also, the simulation results showed that the confining condition has a significant impact on the slope stability when the joint dip angle is increased.

3.4. Stability Analysis of Gravity Dams

Wang et al. [44] proposed a new approach, called the incision body (IB), for contact detection of blocks in 3-D DDA. Using their approach, they studied the stability of a gravity dam on jointed rock foundation and dynamic stability of a fractured gravity dam subjected to earthquake shaking. For this purpose, they considered a typical concrete gravity dam. The dam was 121.5m high and was modeled using three blocks. Four dominant discontinuity sets were considered in rock formation and the dam foundation was simulated with seven blocks. The factor of safety obtained using 3-D DDA and the limit equilibrium method were 3.1 and 3.0, respectively. Also, the authors considered the crack penetrated both the upstream and downstream faces of the Konya dam and

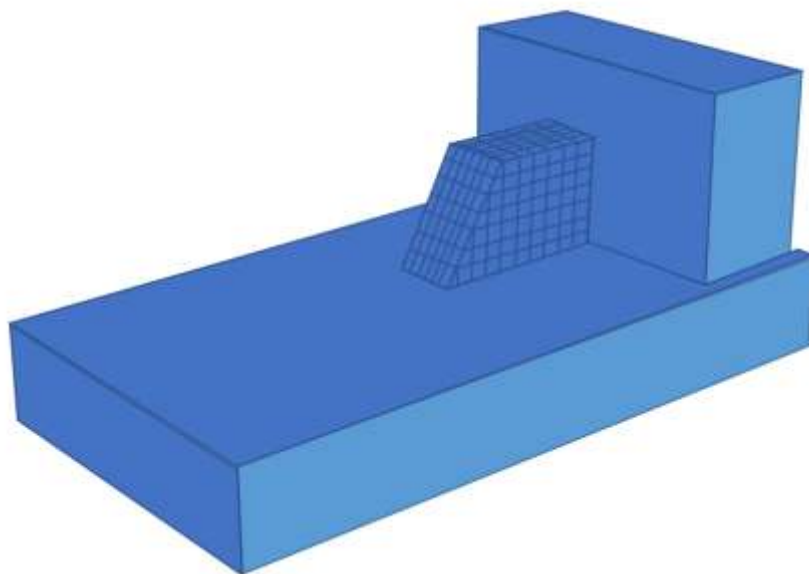


Fig. 3. Initial configuration of 3-D DDA model- free lateral condition (adapted from [43])

analyzed the stability of the dam under Konya earthquake shaking. The results showed that under the earthquake conditions, the dam head part moves to the upstream or the downstream relative to the lower part in a horizontal-cycle mode without bouncing and the relative sliding distance is very small.

3.5. Magma transport through pre-existing fractures

Chen et al. [45] analyzed of magma transport through a pre-existing vertical fracture in the crust by using the combined 3-D DDA, finite difference method (FDM) and finite element method (FEM) approach. For this purpose, they used 3-D DDA to deal with the contact of the closed fracture surfaces and used FDM and FEM to analyze magma flow in the pre-existing fracture and to calculate the opening of the fracture during magma intrusion, respectively. They carried out parametric studies to investigate the influence of various physical and geometric parameters on the magma transport in the pre-existing fracture (i.e., magma chamber depth, magma viscosity, magma density, tectonic stress and fracture breadth). For this purpose, they considered a cuboid above a magma chamber with a pre-existing vertical fracture. The cuboid had a height of $H = 8$ km, a length of 20 km (perpendicular to the fault faces), and a width of 10 km (parallel to the fracture faces). The model sketch is shown in Figure 4. The bottom of the cuboid was fixed along the vertical direction and was free along the horizontal directions. The top of the cuboid was free, and the tectonic stresses were applied to the four side faces of the cuboid. It was found that the depth of magma chamber has a big influence on the minimum overpressure so that the minimum overpressure increases with depth of the magma chamber. They showed that the obtained results are consistent with some field measurements which indicate that their combined numerical technique is an effective tool for simulating magma transport process through pre-existing fractures in the crust.

3.6. In-situ thermal test

Yeung et al. [46] modeled an in-situ thermal test on an exposed block of fractured rock. The test is called the large block test (LBT) and was performed at the Nevada Test Site in the USA. In this test, two multiple point borehole extensometers (MPBXs) were used to measure the anchor point deformations and the temperature histories were measured at various points in the block. In this analysis, the temperature changes were converted to changes in the stresses of the block and were used as input into the 3-D DDA program. The LBT block was cut by five major fractures so that 22 smaller blocks were created. The authors compare the computed and measured anchor point deformations. The comparison showed that in general, the computed MPBX anchor point deformations are in agreement with those of the measured ones.

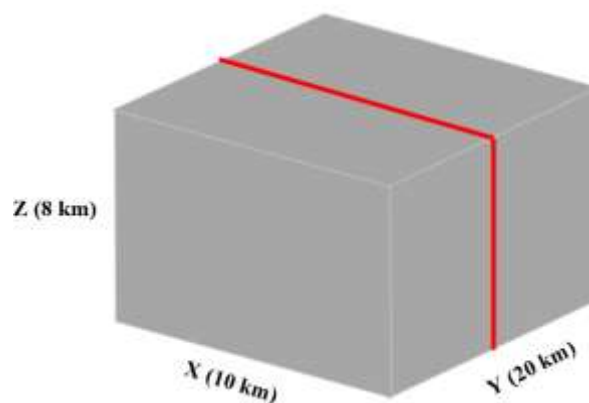


Fig. 4. Sketch of the model used for analyzing magma transport (adapted from [45])

3.7. Damage analysis of brick masonry buildings

In order to simulate the behavior of the brick-mortar structures, Liu et al. [47] developed a block-joint model using 3-D DDA. They used their proposed 3-D DDA model to analyze the velocity distribution and the key point displacements of the brick masonry building under the impact of boulders. For this purpose, they considered seven different types of simplified single-layered masonry building models. They also considered a $1\text{ m} \times 1\text{ m} \times 0.5\text{ m}$ cuboid shape for the boulder with a velocity of 5 m/s to impact all the masonry building models. Based on the obtained results, the authors presented some suggestions such as upgrading the brick and mortar, increasing the wall thickness, making full use of the wall thickness, and adding a circular beam and structural column to improve the impact resistance of a masonry building. No verifications (including comparing the results with physical model tests and field observations) were presented in this study.

Li et al. [48] used 3-D DDA to analyze the 3-D kinetic failure behaviors of brick masonry buildings. They studied six different cases that considered in-plane or out-of-plane boulder impacts to the building at different heights. In order to compare the damage extent of the building, the velocity distribution and several displacements of key points of the building blocks were obtained. Based on the modeling results, it was concluded that the extent of the building damage is related to vertical compressive stress, lateral stiffness, location relationship between the damaged part and impact position, and constraint condition and force condition. In this study, only the influences of the impact direction and impact height were considered. The authors did not study effects of the impact velocity, the boulder size, shape, and elastic modulus, and the angle between the impact direction and horizontal plane.

3.8. Tunnel Stability

Shi [37] used 3-D DDA to analyze an underground powerhouse. Four major joint sets were considered, and total number of the blocks was 7739. In this study, all possible removable blocks were found. However, the authors did not verify the results by comparing them with another method.

Zhu et al. [49] combined 3-D DDA and 3-D binocular photogrammetry for stability analysis of tunnels in jointed blocky rockmass. For this purpose, they considered three modules: (1) photogrammetry module (2) modeling module, and (3) analysis module. In the photogrammetry module, geometric data of jointed blocky rockmass is produced by using binocular photogrammetry devices and image reconstruction technique. In the modeling module, as shown in Figure 5, the 3-D model is generated using the location, dip direction and dip angle of joints and other geometric information of tunnels obtained from the photogrammetry module. Finally, in the analysis module, 3-D DDA is used to analyze the stability of the surrounding rock blocks in tunnels. The authors presented a case study and implemented the 3-D integrated system in a highway tunnel (called Suocaopo Tunnel) in Guizhou, China. The tunnel is 852 m long and was excavated in sandstone and mudstone. Based on the photogrammetry results, 44 joint planes and 181 blocks were generated. Using 3-D DDA, the failure range of surrounding rockmass and the collision range of falling blocks were determined. In this research, the authors did not consider irregular joints and the proposed method is suitable for rockmasses with regular and planar joints.

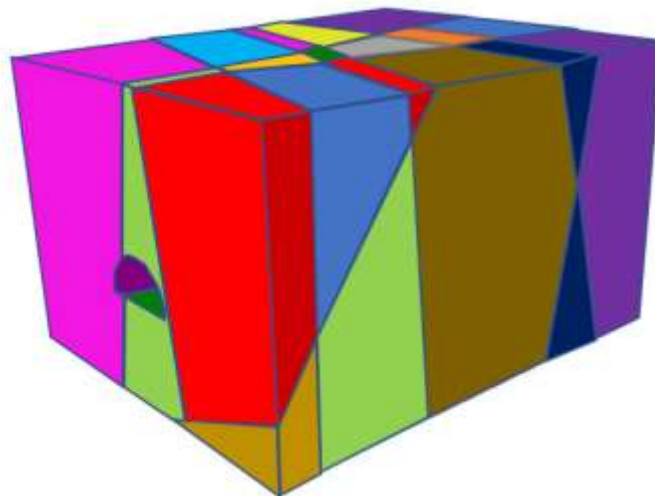


Fig. 4. Blocky model generated in modeling module (adapted from [49])

Su et al. [50] presented a coupling of 3-D DDA and 3-D Finite Element Method (3-D FEM) based on the complementary theory and verified their method by two numerical examples. The coupling method of 3D CDDA-FEM was able to improve the displacement and stress field inside blocks and to describe the large displacement and deformation between rock masses. They used the coupling method to analyze the stability of an underground water diversion and power generation system including nine diversion tunnels, a main power plant, nine busbar tunnels, a main transformer chamber, three surge chambers, and nine tailrace tunnels. The results obtained from the modeling showed that pre-stressed anchor bars can prevent the large displacement and large deformation of the surrounding rock mass.

In order to improve the computing efficiency of 3-D DDA for large-scale simulations, Peng et al. [51] implemented the parallel block Jacobi (BJ) and preconditioned conjugate gradient (PCG) iterative solvers into the original 3D-DDA and showed that the modified 3-D DDA exhibits much higher execution efficiency. The authors analyzed an underground cavern model with two sets of artificial joints with different spacings using both the original and modified 3-D DDA to demonstrate the accuracy and efficiency of their proposed

method. The height and width of the models were 390m and 350m, respectively. The thickness of the models and the number of blocks were 15m and 501, 30m and 998, 45m and 1495, 60m and 1992, and 75m and 2489, respectively. They verified the accuracy of the modified 3-D DDA by comparing the results obtained by both methods. It was shown that the modified 3-D DDA significantly reduces the computing time and provide higher computational efficiency as the number of blocks increases. The reported maximum speedup ratio was up to 5.1.

IV. CONCLUSION

3-D DDA is a relatively new method and has been used for different applications including toppling analysis, rockfall analysis, landslides, stability analysis of gravity dams, magma transport through pre-existing fractures, in-situ thermal test, damage analysis of brick masonry buildings, and tunnel Stability. Based on the material reviewed for this paper, 3-D DDA simulations provide accuracy acceptable for many engineering purposes.

REFERENCES

- [1]. Shi GH. 1988. Discontinuous deformation analysis: a new numerical model for the statics and dynamics of block systems. PhD thesis, Department of Civil Engineering, University of California, Berkeley.
- [2]. Shi GH. 1993. Block System Modeling by Discontinuous Deformation Analysis. Computational Mechanics Publication: Southampton. UK.
- [3]. MacLaughlin MM, Doolin DM. 2006. Review of validation of the discontinuous deformation analysis (DDA) method. *Int J Numer Anal Meth Geomech*, 30: 271–305.
- [4]. Ohnishi Y, Nishiyama S. 2007. Recent insights of analyses using discontinuous methods in rock engineering in Japan. *Proceedings of the 8th International Conference on Analysis of Discontinuous Deformation: Fundamentals and Applications to Mining and Civil Engineering*, Beijing, China, August 14-19, 15–26.
- [5]. Hatzor YH and Bakun-Mazor D. 2011. Modeling dynamic deformation in natural rock slopes and underground openings with DDA: Review of recent results. *Geomechanics and Geoengineering: An International Journal*, 6(4):283–292.
- [6]. Ohnishi Y, Koyama T, Sasaki T, Hagiwara I, Miki S, Shimauchi T. 2012. Application of DDA and NMM to practical problems in recent new insight. *Proceedings of the 11th international conference on analysis of discontinuous deformation*, icadd11, fukuoka, japan, 27–29 august 2013, 31-42.
- [7]. Ohnishi, Y., Sasaki, T., Koyama, T., Hagiwara, I., Miki, S., & Shimauchi, T. 2014. Recent insights into analytical precision and modelling of DDA and NMM for practical problems. *Geomechanics and Geoengineering*, 9(2), 97-112.
- [8]. Yagoda-Biran G, Hatzor Y H. 2016. Benchmarking the numerical Discontinuous Deformation Analysis method, *Computers and Geotechnics*, 71, 30-46.
- [9]. Ning Y, Yang Z, Wei B, et al. Advances in two-dimensional discontinuous deformation analysis for rock-mass dynamics. *Int J Geomech*, 2017, 17:1-11.
- [10]. Shi GH. 2001. Three dimensional discontinuous deformation analysis. *Proceedings of the 38th US Rock Mechanics Symposium*, D Elsworth et al., ed., 1421–1428.
- [11]. Yeung MR, Jiang QH, Sun N. 2003. Validation of block theory and three-dimensional discontinuous deformation analysis as wedge stability analysis method. *Int J Rock Mech Min Sci*, 40(2): 265–275.
- [12]. Liu J, Kong X, Lin G. 2004. Formulation of the three-dimensional discontinuous deformation analysis method. *ActaMechanicaSinica*, 20(3): 270–282.
- [13]. Jiang QH, Yeung MR. 2004. A model of point-to-face contact for three-dimensional discontinuous deformation analysis. *Rock Mechanics and Rock Engineering*, 37(2):95–116.
- [14]. Wu JH, Juang CH, Lin HM. 2005b. Vertex-to-face contact searching algorithm for three-dimensional frictionless contact problems. *International Journal for Numerical Methods in Engineering*, 63(6): 876–897.
- [15]. Yeung MR, Jiang QH, Sun N. 2007. A model of edge-to-edge contact for three-dimensional discontinuous deformation analysis. *Computers and Geotechnics*, 34(3): 175–186.
- [16]. Wu JH. 2008. New edge-to-edge contact calculating algorithm in three-dimensional discrete numerical analysis. *Advances in Engineering Software*, 39(1): 15–24.
- [17]. Beyabanaki SAR, Grayeli R, Hatami K. 2008. Three-dimensional discontinuous deformation analysis (3-D DDA) using a new contact resolution algorithm. *Computers and Geotechnics*, 35: 34356.
- [18]. Beyabanaki SAR, Mikola GR, Biabanaki SO, Mohammadi S. 2009a. New point-to-face contact algorithm for 3-d contact problems using the augmented Lagrangian method. *Geomechanics and Geoengineering: An International Journal*, Taylor & Francis, 4(3): 221–236.
- [19]. Ahn TY, Song JJ. 2011. New contact-definition algorithm using inscribed spheres for 3D discontinuous deformation. *International Journal of Computational Methods*, 8(2): 171–191.
- [20]. Beyabanaki SAR, Jafari A, Biabanaki SO, Yeung MR. 2009b. A coupling model of 3-D discontinuous deformation analysis (3-D DDA) and finite element method, *AJSE*, 34:2B: 107–119.
- [21]. Beyabanaki SAR, Jafari A, Biabanaki SO, and Yeung MR. 2009c. Nodal-based three-dimensional discontinuous deformation analysis (3-D DDA), *Computers and Geotechnics*, 36: 359–372.
- [22]. Beyabanaki SAR, Jafari A, Yeung MR. 2009d. Second-order displacement functions for three-dimensional discontinuous deformation analysis (3-D DDA), *International Journal of Science and Technology*, 16(3): 216–225.
- [23]. Beyabanaki SAR, Jafari A, and Yeung MR. 2010. High-order three-dimensional discontinuous deformation analysis (3-D DDA). *International Journal for Numerical Methods in Biomedical Engineering*, 26 (12): 1522–1547.
- [24]. Beyabanaki SAR, Ferdosi B, Mohammadi S. 2009e. Validation of dynamic block displacement analysis and modification of edge-to-edge contact constraints in 3-D DDA. *International Journal of Rock Mechanics and Mining Sciences*, Elsevier, 46: 1223–1234.
- [25]. Bakun-Mazor D, Hatzor YH, Glaser SD. 2012. Dynamic sliding of tetrahedral wedge: The role of interface friction. *International Journal for Numerical and Analytical Methods in Geomechanics*, 36(3): 327–343.
- [26]. Beyabanaki SAR and Bagtzoglou AC. 2012. Three-dimensional discontinuous deformation analysis (3-D DDA) method for particulate media applications, *Geomechanics and Geoengineering: An International Journal*, 7(4): 239–253.

- [27]. Beyabanaki SAR and Bagtzoglou AC. 2015. Sphere-boundary edge and sphere-boundary corner contacts model in DDA for simulating particulate media in 3-D, *Geomechanics and Geoenvironment: An International Journal*, 10(2): 83–94.
- [28]. Fan H, Zheng H, Zhao J. 2018. Three-dimensional discontinuous deformation analysis based on strain-rotation decomposition, *Computers and Geotechnics* 95: 191–210.
- [29]. Wang X, Wu W, Zhu H, Zhang H, Lin JS. 2020. The last entrance plane method for contact indeterminacy between convex polyhedral blocks, *Computers and Geotechnics* 117: 103283.
- [30]. Hwang JY, Ohnishi Y, Wu J. 2004. Numerical Analysis of Discontinuous Rock Masses Using Three-Dimensional Discontinuous Deformation Analysis (3D DDA), *KSCE Journal of Civil Engineering*, 8: 491–496.
- [31]. Wu JH, Ohnishi Y, Shi GH, Nishiyama S. 2005. Theory of threedimensional discontinuous deformation analysis and its application to a slope toppling at Amatoribashi, Japan. *Int J Geomech*, 179–95.
- [32]. Chen G, Zheng L, Jiang Z. 2012. Comparison of 2D and 3D DDA in rockfall analysis, 46thUS Rock Mechanics / Geomechanics Symposium held in Chicago, IL, USA, 24-27 June 2012, paper ARMA 12-484.
- [33]. Chen GQ, Zheng L, Zhang YB, Wu J. 2013. Numerical simulation in rockfall analysis: a close comparison of 2-D and 3-D DDA. *Rock Mech. Rock. Eng.* 46 (3), 527–541.
- [34]. Sasaki T, Hagiwara I, Miki S, Ohnishi Y, Koyama T. 2012. Studied on rock fall problems by three dimensional discontinuous deformation analysis, *Advances in Discontinuous Numerical Methods and Applications in Geomechanics and Geoenvironment*, Zhao et al. (eds), Taylor & Francis Group, 155-161.
- [35]. Zheng L, Chen GQ, Zen K, Kasama K. 2012. The method of slope modelling for rockfall analysis using 3D DDA, *Advances in Discontinuous Numerical Methods and Applications in Geomechanics and Geoenvironment*, Zhao et al. (eds), Taylor & Francis Group, 189-194.
- [36]. Sasaki T, Hagiwara I, Miki S, Ohnishi Y, Koyama T. 2013. Numerical stability on rock fall problems by 3-D DDA, 47thUS Rock Mechanics / Geomechanics Symposium, ARMA 13-489.
- [37]. Shi GH. 2012. Rock block stability analysis of slopes and underground power houses, *Advances in Discontinuous Numerical Methods and Applications in Geomechanics and Geoenvironment*, Zhao et al. (eds), Taylor & Francis Group, 3-16.
- [38]. Shi GH. 2014. Application of discontinuous deformation analysis on stability analysis of slopes and underground power houses. *Geomechanics and Geoenvironment*, 9: 80-96.
- [39]. Wang W, Chen GQ, Zhang H, Zhou SH, Liu SG, Wu YQ, Fan FS. 2016. Analysis of landslide-generated impulsive waves using a coupled DDA–SPH method, *Engineering Analysis with Boundary Elements*, 64: 267–277
- [40]. Wang W, Chen GQ, Zhang YB, Zheng L, Zhang H. 2017. Dynamic simulation of landslide dam behavior considering kinematic characteristics using a coupled DDA-SPH method. *Engineering Analysis with Boundary Elements*, 80: 172–183.
- [41]. Wang W, Zhang H, Zheng L, Zhang YB, Wu YQ, Liu SG. 2017. A new approach for modeling landslide movement over 3D topography using 3D discontinuous deformation analysis. *Computers and Geotechnics*, 81, 87–97.
- [42]. Zhang H, Liu SG, Wang W, et al. 2016. A new DDA model for kinematic analyses of rockslides on complex 3-d terrain. *Bulletin of Engineering Geology and the Environment*, 1-17.
- [43]. Jing PD, Chen G, Zhang H, Wang W. 2017. Application of Three-Dimensional Discontinuous Deformation Analysis to Simulate Characteristics of Planar Translational Slope Failure. In: *Hazarika H, Kazama M, Lee W. (eds), Geotechnical Hazards from Large Earthquakes and Heavy Rainfalls*. Springer, Tokyo, 339-345.
- [44]. Wang J, Lin G, Liu J. 2006. Static and dynamic stability analysis using 3D-DDA with incision body scheme, *Earthquake Engineering and Engineering Vibration*, 5(2): 273–283.
- [45]. Chen Z, Cheng X, Huang X, Bai W, Jin ZH. 2014. Three-dimensional numerical analysis of magma transport through a pre-existing fracture in the crust, *Journal of Geodynamics* 76: 46–55.
- [46]. Yeung MR, Sun N, Jiang QH, Blair SC. 2004. Analysis of large block test data using three-dimensional discontinuous deformation analysis, *International Journal of Rock Mechanics and Mining Sciences*, 41(3): 458-459.
- [47]. Liu S, Li Z, Zhang H, Wu W, Zhong G, Lou S. 2018. A 3-D DDA damage analysis of brick masonry buildings under the impact of boulders in mountainous areas, *Journal of Mountain Science*, 15(3): 657-671.
- [48]. Li Z, Liu S, Zhang H, et al. 2018. Simulating the damage extent of unreinforced brick masonry buildings under boulder impact using three-dimensional discontinuous deformation analysis (3-D DDA), *Engineering Failure Analysis*, 93: 122–143.
- [49]. Zhu HH, Wu W, Chen JQ, Ma GW, Liu XG, Zhang XY. 2016. Integration of three dimensional discontinuous deformation analysis (DDA) with binocular photogrammetry for stability analysis of tunnels in blocky rockmass. *Tunnelling and Underground Space Technology*, 51: 30–40.
- [50]. Su C, Ren ZM, Dao VH, Dong YJ. 2018. A Coupling of Three-Dimensional Finite Element Method and Discontinuous Deformation Analysis Based on Complementary Theory, In: *Nguyen-Xuan H, Phung-Van P, Rabczuk T. (eds), In Proceedings of the International Conference on Advances in Computational Mechanics 2017*, 955-973
- [51]. Peng X, Chen G, Yu P, Zhang Y, Guo L, Wang C. 2019. Parallel computing of three-dimensional discontinuous deformation analysis based on OpenMP, *Computers and Geotechnics* 106: 304–313.

S. Amir Reza Beyabanaki" Applications of Three-Dimensional Discontinuous Deformation Analysis: A Review" *American Journal of Engineering Research (AJER)*, vol. 8, no. 10, 2019, pp 237-245